



# Influence of dc magnetron sputtering parameters on surface morphology of indium tin oxide thin films

Yeon Sik Jung<sup>a,\*</sup>, Dong Wook Lee<sup>a</sup>, Duk Young Jeon<sup>b</sup>

<sup>a</sup>R&D Center, Samsung Corning, 644, Jinpyoung-dong, Gumi, Kyoung-buk 730-725, South Korea

<sup>b</sup>Department of Materials Science and Engineering, Korea Advanced Institute of Science and Technology, 373-1, Kusong-dong, Yusung-gu, Taejon 305-701, South Korea

Received 3 May 2003; received in revised form 25 June 2003; accepted 26 June 2003

## Abstract

Indium tin oxide (ITO) thin films were prepared by dc magnetron sputtering deposition on glass substrates under different process conditions. The surface morphology was monitored using atomic force microscopy (AFM) and scanning electron microscopy (SEM). The change in surface morphology of ITO films was discussed in terms of crystallographic orientation and grain size. The crystallographic orientations and the grain sizes of the samples significantly changed with different sputtering parameters. Moderate ranges of pressure and power density, less amounts of additional oxygen gas, and higher substrate temperatures, where adatoms are expected to have higher mobility, resulted in a rougher surface. Under those conditions, the domains had more mixed orientations, and the average sizes of grains were larger.

© 2003 Elsevier B.V. All rights reserved.

PACS: 68.55.Jk structure and morphology, crystalline orientation and texture; 81.15.Cd deposition by sputtering; 68.37.Ps atomic force microscopy (AFM)

Keywords: Indium tin oxide; Sputtering; Morphology; Atomic force microscopy

## 1. Introduction

Many kinds of transparent conducting oxide (TCO) films such as impurity-doped indium oxides, tin oxides, and zinc oxide systems have been widely used as transparent conductors for numerous opto-electronic applications [1–3]. Especially indium tin oxide (ITO) thin films have been widely used due to low resistivity, high transmittance, and good etching properties [4,5].

The surface roughness of thin films has been reported to influence the electrical and optical properties [6,7]. Recently, organic light emitting diodes (OLEDs), which are one of the most promising candidates for flat panel displays, demand a very flat surface of TCOs. In general, homogeneity and surface roughness are very important for the reliability of the devices since the organic layers in OLEDs have thicknesses of only about 100 nm [8]. Especially, the peak-to-valley roughness of ITO films has a linear relationship with the reverse leakage current of the devices [9]. Also, the surface morphology of ITO films considerably affects the patterning properties during the fabrication process of flat panel displays [10].

\* Corresponding author. Tel.: +82-54-470-7494;  
fax: +82-54-470-7814.  
E-mail address: [ysjung@bomun.kaist.ac.kr](mailto:ysjung@bomun.kaist.ac.kr) (Y.S. Jung).

ITO films deposited with RF magnetron sputtering, ion plating, and pulsed laser deposition (PLD) have been reported to have a very flat surface and also outstanding properties [11–13]. On the other hand, dc magnetron sputtering deposition technique has been commonly used to deposit ITO thin films of fine electrical and optical properties [14,15]. Since dc magnetron sputtering techniques have the advantage of much better productivity than other deposition methods, it is widely used as mass production processes. Thus, it is thought to be valuable to elucidate the factors influencing the surface roughness of ITO thin films depending upon dc magnetron sputtering parameters.

In this paper, we report on the factors controlling the surface morphology of ITO films deposited with dc magnetron sputtering deposition. Characterization tools such as X-ray diffraction (XRD), scanning electron microscopy (SEM) and atomic force microscopy (AFM) were used to monitor the variation of the surface morphology and the structural properties of ITO films with deposition parameters.

## 2. Experiment

ITO thin films were sputter-deposited using an ITO target in an in-line magnetron sputter-deposition system equipped with dc power suppliers. The chamber, which was equipped with a load-lock system and diffusion pumps, had a base pressure of  $6 \times 10^{-4}$  Pa. The target (128 mm  $\times$  450 mm) used was a sintered ITO containing 10 wt.% SnO<sub>2</sub> (99.99%). Sputtering was carried out at a pressure of 0.1–3 Pa in pure Ar or Ar/O<sub>2</sub> gas mixture with varying sputtering parameters such as sputtering pressure, power density, oxygen flow rate and deposition temperature. The deposition temperature was usually 200 °C except the samples to investigate the effect of temperature. The films were deposited on non-alkali glass (Corning 1737), which were placed 50 mm apart and parallel from the target surface. The substrates were cleaned in an ultrasonic bath containing a detergent (Deconex 12PA) at 65 °C for 6 min, and then rinsed in deionized water in the ultrasonic bath for another 15 min. The cleaned substrates were dried at 100 °C for 15 min. The target was pre-sputtered for 3 min. The thickness of the deposited films was about 150 nm.

Conventional  $\theta$ – $2\theta$  X-ray diffraction studies on the films were carried out in a Philips PW1710 diffractometer using Cu K $\alpha$  radiation ( $\lambda = 1.5405\text{\AA}$ ). Surface roughness was determined and three-dimensional images were taken by atomic force microscopy (AFM, Auto-probe M5, PSIA Co.). Also, field emission scanning electron microscopy (FESEM, JSM 6700F, JEOL) was used to observe the surface image of samples. The ITO films deposited with ion plating (Sumitomo Heavy Industries) were analyzed together to compare their properties with those of samples prepared by dc magnetron sputtering.

## 3. Results and discussion

Fig. 1(a) shows an SEM image of conventional ITO films deposited at 200 °C with a dc magnetron sputtering technique. The image shows a characteristic surface morphology, which is known as a grain-subgrain structure (or domain-grain structure) [10]. In this study, we follow nomenclature of domain-grain, where large angle grain boundaries are called as domain boundaries. Shigesato and Paine proposed that those types of morphology are caused by ion bombardment during sputtering deposition [16]. Kamei et al. claimed that higher durability of (4 0 0) planes against re-sputtering during film growth

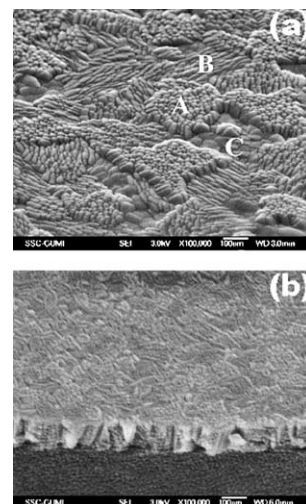


Fig. 1. Typical SEM images of ITO thin films deposited by (a) a dc magnetron sputtering and (b) an ion plating at 200 °C.

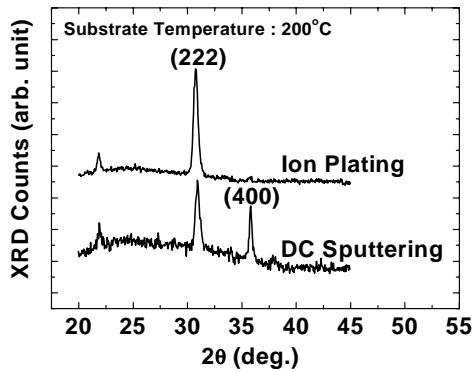


Fig. 2. XRD spectra of the ITO films deposited by an ion plating and a dc magnetron sputtering.

results in the difference in the height of domains with different orientations [10]. The difference in height seems to be a factor in describing surface roughness of ITO films. The domains A–C with different morphology, as shown in Fig. 1, have different height, and thus many protrusions and steps are expected to be formed on the surface. Actually, the ITO films deposited with ion plating deposition, which have (2 2 2) preferred orientation as shown in Fig. 2, do not have significant difference in the height of domains as shown in Fig. 1(b), thus show a very smooth surface. The measured root-mean-square roughness ( $R_{\text{rms}}$ ) value by AFM was 7–9 Å, which is much smaller than that of the ITO films deposited with dc magnetron sputtering technique. The samples sputter-deposited at the same deposition temperature of 200 °C had mixed orientations, and their  $R_{\text{rms}}$  values was 20–40 Å.

Fig. 3 presents the AFM images of the samples deposited under different pressure. The samples were deposited without supplying additional oxygen gas to avoid the influence of different oxygen gas content in the films. The morphology of the samples significantly varied with different sputtering pressures. In the moderate pressure (0.15 Pa), larger sizes of grains were observed. To quantify the grain size, the number of grains per unit area ( $1 \mu\text{m}^2$ ) was counted in Fig. 4(b). Higher number of grains means the average grain size is smaller. The number of grains was lower for the sample deposited at about 0.15 Pa.

Many researchers have reported the relationship between the grain size of ITO films and the energy of ions during sputtering. Yang et al. reported that the

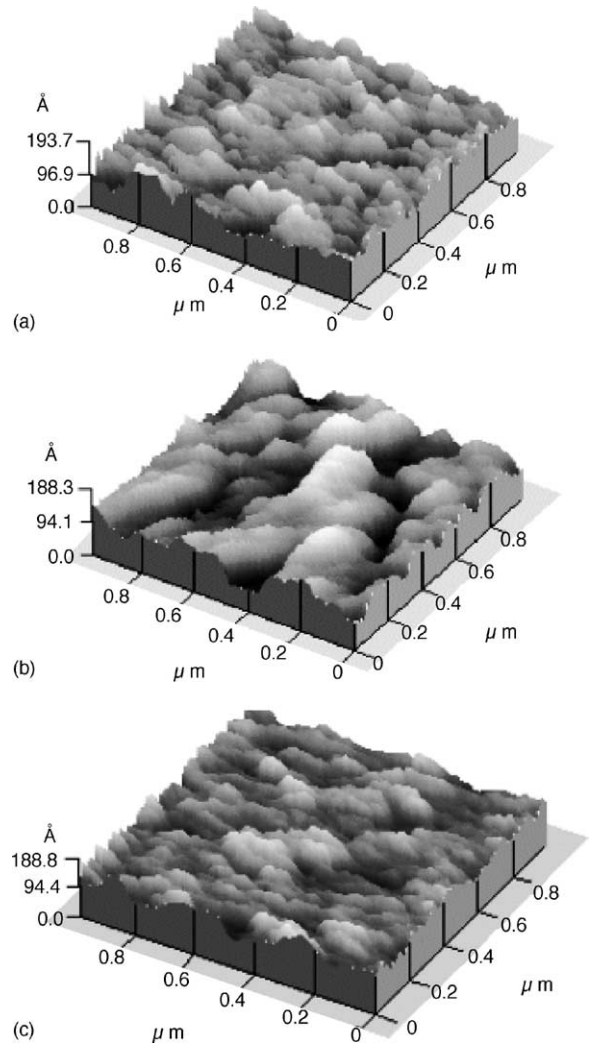


Fig. 3. AFM images of the surface of the ITO films deposited at (a) 0.1 Pa; (b) 0.15 Pa and (c) 1.4 Pa.

grain size was larger in moderate range of negative bias voltage [17]. It was presented that ion beam energy could increase the grain size under a low energy condition due to increased adatom mobility, however, too higher energy decreased the grain size [18,19]. Y. Shigesato presented that the initial growth stage of ITO thin films is a Volmer–Weber type [20], where islands are formed before the formation of a continuous film. Coalescence at the initial stage of film growth decreases density of the island [21], which means that smaller number of grains appears on sur-

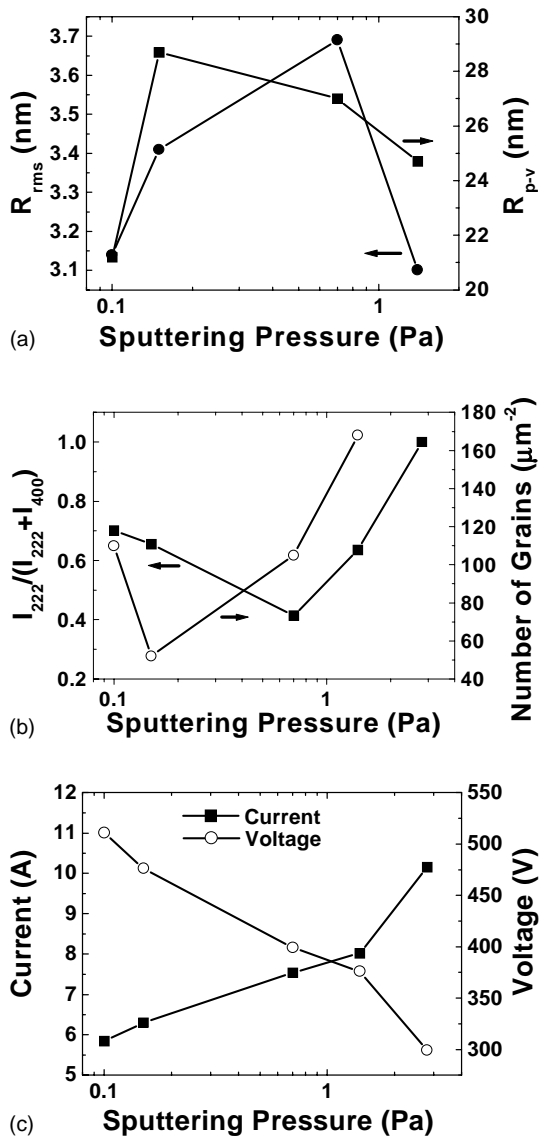


Fig. 4. Changes of (a) roughness values measured by AFM; (b) relative portion of (2 2 2)-peak intensity measured by XRD and the number of grains per unit area measured by an AFM and (c) discharge voltage and current depending upon sputtering pressure.

face after coalescence. Hence, the films deposited under the conditions for promoting coalescence will have larger grains. Chiu and Barber proposed that the product of ion flux and incident energy represents the resultant energy supplied by ion bombardment per unit number of deposited atoms [22]. At a very high

pressure, lower ion energy due to the frequent collisions among neutral gases and ions results in very low adatom mobility. In the case of lower adatom mobility, the coalescence process is more kinetically limited than in the case of higher adatom mobility. Consequently, low adatom mobility under high sputtering pressure leads to smaller islands at the initial stage and therefore smaller grains later. However, in the moderate range of pressure (0.15–0.7 Pa), where adatoms obtain more energy by ion bombardment, the adatoms can move more actively, and larger grains are formed. On the other hand, at a low sputtering pressure, the discharge voltage is much higher than other conditions as shown in Fig. 4(c). When the discharge voltage is high (several 100 eV) during the sputtering deposition of ITO films, negative oxygen ions bombard the film with higher energy, and consequently the high-energy ions damage the film [23]. Furthermore, the high-energy particles have sufficient energy to perturb the growth of ITO films by displacing surface atoms [23]. Therefore, the size of initially formed nuclei would be small when deposited at a low pressure due to the etching effect by high-energy negative ions.

Higher adatom mobility led to more (4 0 0) orientation, as shown in Fig. 4(b). Though the relative portion of (2 2 2)-peak intensity ( $I_{(222)}/(I_{(222)} + I_{(400)})$ ) is not exactly same as the true portion of (2 2 2)-oriented domains, it could be an indirect measure of the portion. The intensity of each peak was measured by fitting and integrating a Gaussian function. The resultant roughness values are shown in Fig. 4(a). The roughness values were acquired from much larger area ( $20 \mu\text{m} \times 20 \mu\text{m}$ ), thus the values will be influenced by the average grain sizes as well as the height difference among the domains with different orientations. The definition of  $R_{\text{rms}}$  is the root-mean-square value of the surface roughness profile from the centerline, and peak-to-valley roughness ( $R_{\text{p-v}}$ ) is the vertical distance between the highest and lowest points [9]. Fig. 4(a) shows that the roughness values were higher in the moderate range of sputtering pressure (0.15–0.7 Pa). However, the highest point of the  $R_{\text{rms}}$  was different from that of the  $R_{\text{p-v}}$ . The  $R_{\text{p-v}}$  value was highest at 0.15 Pa, where the grain size was largest. The  $R_{\text{rms}}$  value was highest at 0.7 Pa, where the portion of (4 0 0) domain was highest. Of course, the values are closely related with each other, but each value can describe

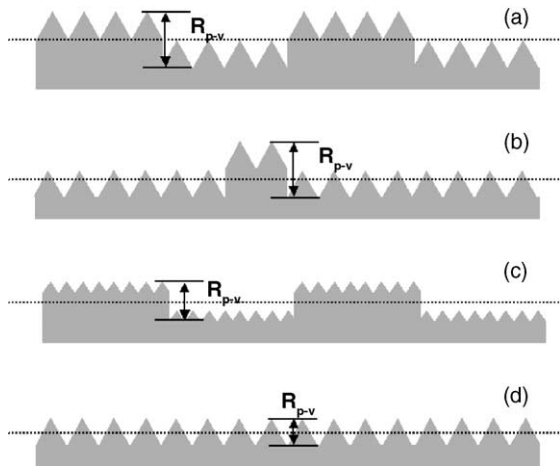


Fig. 5. Schematic diagrams of cross-section view of ITO morphology.

more specific morphology. These results mean that the  $R_{p-v}$  value depends on mainly the size of grains, and the  $R_{rms}$  follow basically the uneven surface caused by the height difference of domains.

Fig. 5 presents several simplified cases that cause the difference in surface roughness with different domain orientations and grain sizes. The schematic diagrams of cross-sectional ITO morphology shown in Fig. 5(a) and (b) have the same grain size and different combination of domain orientation. The height difference among the domains with different orientations was assumed to be constant. In such a case,  $R_{p-v}$  may not change significantly since the heights of the highest point and the lowest point are similar, while  $R_{rms}$  will be lower in the case of Fig. 5(b) than (a) since the deviated area from the center line is smaller for Fig. 5(b). However, if the domains have a perfect orientation like Fig. 5(d), the  $R_{p-v}$  value as well as the  $R_{rms}$  value will be considerably lowered. The morphology shown in Fig. 5(a) and (c) have the same combination of domain orientation and different grain size. The  $R_{p-v}$  value is apparently lower in Fig. 5(c), while  $R_{rms}$  is similar or slightly lower for Fig. 5(a) if the height difference among the domains with different orientations is assumed to be similar for the two cases. These models and explanations can support more dependence of  $R_{rms}$  on domain orientations and that of  $R_{p-v}$  on grain sizes.

Fig. 6(a) shows that both the  $R_{rms}$  and the  $R_{p-v}$  values were higher in the moderate range of sputtering

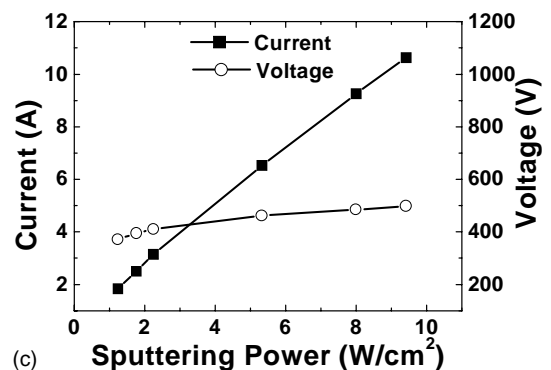
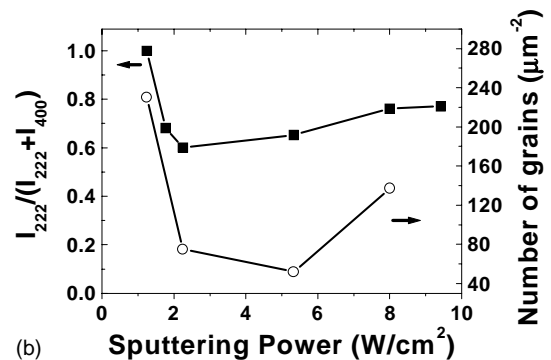
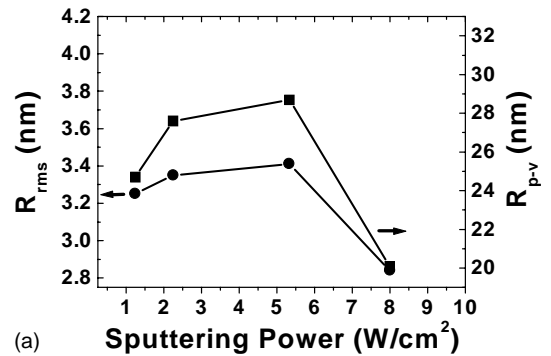


Fig. 6. Changes of (a) roughness values measured by AFM; (b) relative portion of (2 2 2)-peak intensity measured by XRD and the number of grains per unit area measured by AFM and (c) discharge voltage and current depending upon power density.

power density (2–6  $W/cm^2$ ). The samples were deposited without supplying additional oxygen gas with the deposition temperature of 200 °C. The sputtering pressure was 0.15 Pa. As shown in Fig. 6(a), the grain size was larger, and the portion of (4 0 0)-oriented domains was higher in the range. At a low sputtering

power density, the target current is considerably low as shown in Fig. 6(a), which means lower ion bombardment effect due to lower ion flux into the deposited film during sputtering deposition. The discharge voltage is also relatively lower at a low sputtering power condition. Consequently, adatom mobility is expected to be quite low at very low sputtering power density. Actually, the crystallinity of the sample deposited at a very low power density was bad. Its XRD profile showed only a very weak (2 2 2) peak. Adatom mobility will increase with increasing sputtering power density. However, at higher power densities than a critical point, the possibility that the adatoms find thermodynamically favorable sites will decrease due to the increased shadowing effect with deposition rate. In this study, the dynamic deposition rate increased approximately from 60 to 400 nm × m/min when the power density changed from 1.24 to 8 W/cm<sup>2</sup>. The diffusion length (or time) of adatoms will be diminished at high power density since the adatoms are more likely to be buried by incident sputtered atoms before the adatoms find thermodynamically favorable sites. Consequently, the grain size was relatively higher in the moderate range of sputtering power density (2–6 W/cm<sup>2</sup>), where the adatom mobility is thought to be higher. The increase in the portion of (4 0 0)-oriented domains in the range is also attributed to higher adatom mobility. As a result, the ITO samples deposited at very low and high power density, where domains are more (2 2 2)-oriented and grains are smaller, showed a relatively smoother surface.

Fig. 7(a) presents that both the  $R_{\text{rms}}$  and the  $R_{\text{p-v}}$  values decrease with increasing oxygen flow rate. The other deposition conditions such as pressure, power and temperature were fixed. The samples were deposited at 200 °C. The sputtering pressure was 0.15 Pa, and the sputtering power density was 5.33 W/cm<sup>2</sup>. These results can be explained from the grain size and the relative portion of (2 2 2)-peak intensity shown in Fig. 7(b). The grains became smaller and more (2 2 2)-oriented in the samples deposited with higher oxygen gas flow rate. With increased oxygen partial pressure during sputtering, more oxygen atoms would be absorbed on the substrate or film surface. As a result, the In and Sn metal adatoms are likely to be easily trapped by the oxygen atom, and the average adatom mobility and diffusion length will decrease under high

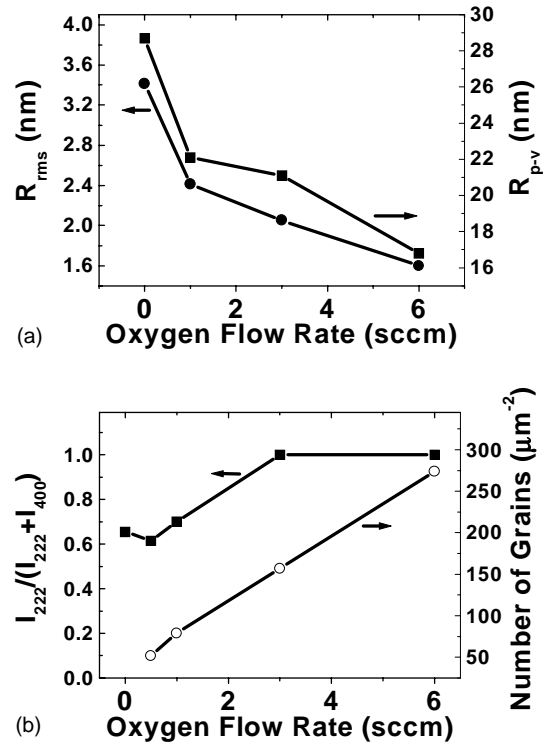


Fig. 7. Changes of (a) roughness values measured by AFM and (b) relative portion of (2 2 2)-peak intensity measured by XRD and the number of grains per unit area measured by AFM depending upon oxygen flow rate.

oxygen partial pressure. Thus, the coalescence step will be more kinetically limited, and the resultant size of grains will be smaller. The dominance of (2 2 2) peak at high oxygen flow rate during the deposition of ITO films has been reported by many researchers [24,25]. The dominance of (2 2 2) peak also contributed to a lower roughness value.

Fig. 8(a) shows that both the  $R_{\text{rms}}$  and the  $R_{\text{p-v}}$  values were larger at higher deposition temperature. The samples were deposited without supplying additional oxygen gas. The sputtering pressure was 0.15 Pa, and the sputtering power density was 5.33 W/cm<sup>2</sup>. As shown in Fig. 8(b), the grain size was larger and the portion of (4 0 0)-oriented domains was higher at elevated temperatures. Substrate temperature can be a direct measure for adatom mobility. At high temperature, the adatoms would have sufficient activation energy for the coalescence of nuclei formed. The dominance of (4 0 0) peak at high

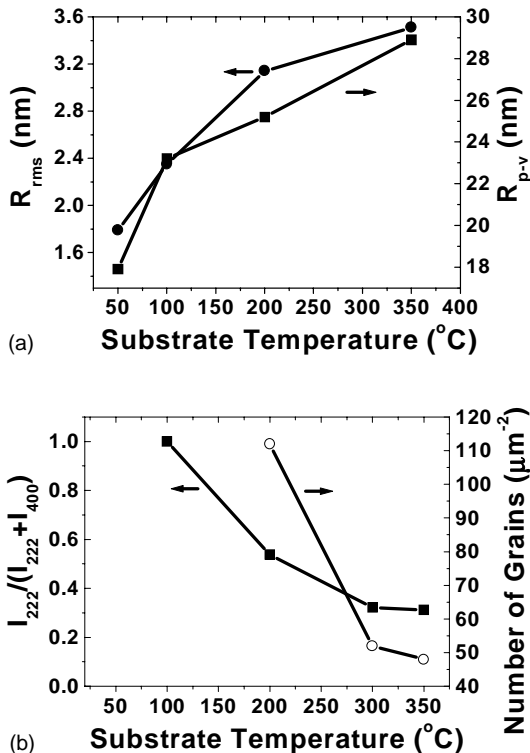


Fig. 8. Changes of (a) roughness values measured by AFM and (b) relative portion of (2 2 2)-peak intensity measured by XRD and the number of grains per unit area measured by AFM depending upon deposition temperature.

deposition temperature has been also reported by other researchers [26].

#### 4. Conclusion

The change in surface morphology of ITO films deposited with dc magnetron sputtering was analyzed in terms of crystallographic orientation and grain size. The crystallographic orientations and the grain sizes of the samples were considerably varied with different sputtering parameters. Less amounts of additional oxygen gas, moderate ranges of pressure and power density and higher substrate temperatures, where adatoms are expected to have higher mobility, resulted in a rougher surface. Under those conditions, the domains had more mixed orientations, and the average sizes of grains were larger.

#### Acknowledgements

The authors acknowledge Moo Sung Lee for SEM and AFM analysis.

#### References

- [1] G. Haacke, *Annu. Rev. Mater. Sci.* 7 (1977) 73.
- [2] C.G. Granqvist, *Appl. Phys. A* 52 (1991) 83.
- [3] H. Sato, T. Minami, S. Takata, T. Miyata, M. Ishii, *Thin Solid Films* 102 (1983) 1.
- [4] I. Hamberg, C.G. Granqvist, *J. Appl. Phys.* 60 (1986) R123.
- [5] S. Ishibashi, Y. Higuchi, Y. Ota, K. Nakamura, *J. Vac. Sci. Technol. A* 8 (1990) 1403.
- [6] J. Yu, X. Zhao, Q. Zhao, G. Wang, *Mater. Chem. Phys.* 68 (2001) 253.
- [7] T. Ishihara, K. Matsuzawa, M. Takayanagi, S. Takagi, *Jpn. J. Appl. Phys.* 41 (2002) 2353.
- [8] CH. Jonda, A.B.R. Mayer, U. Stolz, *J. Mater. Sci.* 35 (2000) 5645.
- [9] Y.H. Tak, K.B. Kim, H.G. Park, K.H. Lee, J.R. Lee, *Thin Solid Films* 411 (2002) 12.
- [10] M. Kamei, Y. Shigesato, S. Takaki, *Thin Solid Films* 259 (1995) 38.
- [11] K. Zhang, F. Zhuh, C. Huan, A. Wee, *Thin Solid Films* 376 (2000) 255.
- [12] Y. Suzuki, F. Niino, K. Katoh, *J. Non-Cryst. Solids* 218 (1997) 30.
- [13] H. Kim, C.M. Gilmore, A. Pique, J.S. Horwitz, H. Mattoussi, H. Murata, Z.H. Kafafi, D.B. Chrisey, *J. Appl. Phys.* 86 (1999) 6451.
- [14] J. Kanazawa, T. Haranoh, K. Matsumoto, *Vacuum* 41 (1990) 1463.
- [15] T. Minami, H. Sonohara, T. Kakumu, S. Takata, *Thin Solid Films* 270 (1995) 37.
- [16] Y. Shigesato, D.C. Paine, *Thin Solid Films* 238 (1994) 44.
- [17] Z.W. Yang, S.H. Han, T.L. Yang, L. Ye, D.H. Zhang, H.L. Ma, C.F. Cheng, *Thin Solid Films* 366 (2000) 4.
- [18] D.V. Morgan, A. Salehi, Y.H. Aliyu, R.W. Bunce, D. Diskett, *Thin Solid Films* 258 (1995) 283.
- [19] D. Kim, S. Kim, *Surf. Coat. Technol.* 154 (2002) 204.
- [20] Y. Shigesato, R. Koshi-ishi, T. Kawashima, J. Ohsako, *Vacuum* 59 (2000) 614.
- [21] M. Ohring, *The Materials Science of Thin Films*, San Diego, Academic Press, 1992.
- [22] K.-F. Chiu, Z.H. Barber, *Thin Solid Films* 358 (2000) 264.
- [23] Y. Shigesato, D.C. Paine, *Thin Solid Films* 238 (1994) 44.
- [24] J.E. Green, J.-F. Sundgren, L. Hultman, I. Petrov, D.B. Bergstrom, *Appl. Phys. Lett.* 67 (1995) 2928.
- [25] H. Izumi, F.O. Adurodija, T. Kaneyoshi, T. Ishihara, *J. Appl. Phys.* 91 (2002) 213.
- [26] C.G. Choi, K.No, W.J. Lee, H.G. Kim, S.O. Jung, W.J. Lee, W.S. Kim, S.J. Kim, C. Yoon, *Thin Solid Films* 258 (1995) 274.